

## Hydrogen spillover boosts PET upcycling to aviation fuel additives over Co–ReO<sub>x</sub> catalysts

*Xin Zhao,<sup>1#</sup> Hui Wang,<sup>1#</sup> Zhecheng Fang,<sup>2</sup> Zixu Ma,<sup>1</sup> Shuzhuang Sun,<sup>1,\*</sup> Dan Wu,<sup>1</sup> Yongsheng Zhang,<sup>1</sup> Chunbao Charles Xu,<sup>4</sup> Shengyong Lu,<sup>3</sup> Renfeng Nie,<sup>1\*</sup> Jie Fu<sup>2,5\*</sup>*

<sup>1</sup> National Key Laboratory of Biobased Transportation Fuel Technology, School of Chemical Engineering, Zhengzhou University, Zhengzhou, 450001.

<sup>2</sup> Key Laboratory of Biomass Chemical Engineering of Ministry of Education, College of Chemical and Biological Engineering, Zhejiang University, Hangzhou, 310028.

<sup>3</sup> State Key Laboratory for Clean Energy Utilization, Institute for Thermal Power Engineering, Zhejiang University, Hangzhou, 310028.

<sup>4</sup> School of Energy and Environment, City University of Hong Kong, Kowloon, Hong Kong SAR

<sup>5</sup> Zhejiang Key Laboratory of Green Biomanufacturing of Functional Sugar Alcohols, Institute of Zhejiang University-Quzhou, 99 Zheda Road, Quzhou 324000, China

Corresponding Authors: [rnie@zzu.edu.cn](mailto:rnie@zzu.edu.cn) (R.N.), [jiefu@zju.edu.cn](mailto:jiefu@zju.edu.cn) (J. F.), [ssun@zzu.edu.cn](mailto:ssun@zzu.edu.cn) (S. S.)

## 1. Experimental section

### 1.1 Materials

PET powder was obtained by cutting up PET water bottle (Cestbon). Dimethyl terephthalate (DMT, 99%) was purchased from Shanghai Aladdin Biochemical Technology Co., Ltd.  $\text{Co}(\text{NO}_3)_2 \cdot 6\text{H}_2\text{O}$  (99%),  $\text{Ni}(\text{NO}_3)_2 \cdot 6\text{H}_2\text{O}$  (98%),  $\text{Al}(\text{NO}_3)_3 \cdot 9\text{H}_2\text{O}$  (99%),  $\text{NH}_4\text{ReO}_4$  ( $\geq 99\%$ ), urea (99%), p-xylene (PX, AR), methylcyclohexane (MCH, 99%), 1,4-dimethylcyclohexane (DMCH, 98%), methyl benzoate (MB, 98%), toluene (PT, 99.5%), tridecane (98%), methanol (99.5%), and 2-PrOH (99.7%) were purchased from Shanghai Maclin Biochemical Technology Co., Ltd. All chemicals were used directly without further purification.

### 1.2 Catalyst preparation

CoAl-LDO was prepared using a hydrothermal synthesis procedure. Specifically, 5 mmol  $\text{Co}(\text{NO}_3)_2 \cdot 6\text{H}_2\text{O}$ , 10 mmol  $\text{Al}(\text{NO}_3)_3 \cdot 9\text{H}_2\text{O}$ , and 70 mmol urea were added to 50 mL deionized water and stirred at room temperature until a clear solution was formed. The solution was then transferred to an autoclave and heated at 140 °C for 9 h. After cooling to room temperature, the resulting solid slurry was filtered, washed, and dried under vacuum at 60 °C, denoting as CoAl-LDO. Subsequently, the solid material was calcined at 500 °C for 5 h followed by reducing in a  $\text{H}_2$  atmosphere at 600 °C for 1 h.

For the preparation of Co/ReO<sub>x</sub>-LDO catalysts, 500 mg CoAl-LDO was dispersed in 10 mL deionized water along with a certain amount of  $\text{NH}_4\text{ReO}_4$  and stirred for 30 min. The water was then removed via rotary evaporation, and the solid powder was obtained by vacuum drying at 60 °C. Subsequently, the solid material was calcined at 500 °C for 5 h followed by reducing in a  $\text{H}_2$  atmosphere at 600 °C for 1 h. The amounts of  $\text{NH}_4\text{ReO}_4$  were adjusted to 18, 36, 72, and 108 mg, denoting as Co/ReO<sub>x</sub>-LDO-2.5, Co/ReO<sub>x</sub>-LDO-5, Co/ReO<sub>x</sub>-LDO-10, and Co/ReO<sub>x</sub>-LDO-15, respectively. The ReO<sub>x</sub>/Al<sub>2</sub>O<sub>3</sub> was prepared using commercial Al<sub>2</sub>O<sub>3</sub> as the support *via* a similar procedure as for Co/ReO<sub>x</sub>-LDO.

### 1.3 Characterizations

The crystal structures of the catalysts were analyzed using powder X-ray diffraction

(XRD) on a Bruker D8 Advance X-ray diffractometer (Bruker, Germany) with Co K $\alpha$  radiation in a scan range of 10–80°. The Raman spectra were recorded at room temperature using a 514.5 nm Ar ion laser (Renishaw Instruments) within the range of 100–4000 cm<sup>-1</sup>. N<sub>2</sub> adsorption-desorption isotherms were measured at -196 °C using a Micromeritics ASAP 2460 analyzer. Total pore volume was determined from N<sub>2</sub> adsorption at a relative pressure of 0.99. Specific surface area was calculated using the BET method, and pore size distribution was obtained from the adsorption branch of the isotherm using the BJH method. The morphology of the catalyst was monitored on a JEM2100F electron microscope (JEOL, Japan) with an acceleration voltage of 200 kV and a resolution of 1.4 Å for transmission electron microscopy (TEM) studies.

Co and Re loadings of the catalysts were analyzed using inductively coupled plasma optical emission spectrometry (ICP-OES, Thermo Scientific ICAP PRO X). The X-ray photoelectron spectroscopy (XPS) was conducted on an Escalab 250Xi spectrometer (Thermo Scientific) equipped with an Al K $\alpha$  X-ray source (1486.6 eV) operating at 300 W (12 kV/25 mA). The detection limit was 1 at% and all binding energies were referenced to the C1s peak at 284.8 eV.

H<sub>2</sub>-TPD was conducted using an AutoChem II 2920 equipped with a TCD. A 0.1 g sample was reduced at 600 °C under H<sub>2</sub> flow (10 °C/min) for 1 h, cooled to 30 °C, and exposed to 10% H<sub>2</sub>/He for 30 min. After purging with He for 1 h to remove physisorbed H<sub>2</sub>, desorption was monitored during heating to 600 °C at 10 °C/min.

The reduction behavior of Co was investigated by H<sub>2</sub>-TPR. A 0.05 g catalyst sample, after pretreatment at 200 °C under He flow, was subjected to H<sub>2</sub>-TPR using a 10% H<sub>2</sub>/Ar flow (20 mL/min) at a heating rate of 5 °C/min to 800 °C. The TCD signal was recorded.

The Electron Paramagnetic Resonance (EPR) analysis was conducted using a Bruker X-band CW EPR spectrometer.

Pyridine-FTIR spectroscopy (PerkinElmer GX) was performed as follows: A 15 mg catalyst/15 mg KBr pellet, after vacuum pretreatment at 300 °C for 1 h, was exposed to pyridine at 30 °C for 1 h, followed by treatments at 50, 100, and 150 °C (each for 1 h).

The Co K-edge X-ray absorption spectroscopy data were collected using a bench-top

easyXAFS300+ instrument (easyXAFS, LLC). Spectra were collected using Si spherically bent crystal analyzer and Ag anode X-ray tube, respectively. Spectra were deadtime corrected and the energy was calibrated using a Co foil standard.

The hydrogen spillover was monitored in situ using diffuse reflectance infrared Fourier transform spectroscopy (DRIFTS). The experiments were conducted on a Bruker Tensor 27 spectrometer equipped with an in-situ reaction chamber and a liquid nitrogen-cooled high-sensitivity mercury cadmium telluride (MCT) detector. Typically, ~ 20 mg of finely ground catalyst was placed in the reaction chamber and reduced in a 10% H<sub>2</sub>/Ar atmosphere at 673 K for 1 h. After cooling the sample to room temperature, hydrogen was introduced into the reaction chamber for 5 mins followed by purging with helium. Time-resolved spectra were recorded with a resolution of 4 cm<sup>-1</sup> and an accumulation of 128 scans, compared against an appropriate background spectrum.

In-situ DRIFTS experiments were conducted using a Bruker Invenio S equipped with Harrick optical accessories, a DRIFTS cell featuring ZnSe windows, and a mercury cadmium telluride (MCT) detector. The IR signal was collected over a range of 4000 to 400 cm<sup>-1</sup> with a resolution of 4 cm<sup>-1</sup>. Two sets of in-situ DRIFTS experiments were performed: one for H spillover verification and the other for ethyl acetate adsorption-hydrogenation. For the H spillover verification, the Co and CoRe catalysts were initially reduced in situ at 400 °C for 1 h in H<sub>2</sub>, followed by annealing in Ar at 550 °C to eliminate surface-adsorbed H. The catalyst was then cooled to the test temperature in Ar, and the background was recorded. Subsequently, IR spectra were collected after introducing a 30 mL/min flow of H<sub>2</sub> to assess the H spillover effect at specific temperatures. The H spillover effect was evaluated within a temperature range of 100 to 400 °C, with increments of 50 °C.

Ethyl acetate was used as a model compound to evaluate the reduction of carbonyl groups over various catalysts. For the ethyl acetate adsorption-hydrogenation, the Co and CoRe catalysts were *in-situ* reduced using the same procedure as described above. The catalysts were then cooled to 300 °C in Ar, and the background spectrum was collected. Ethyl acetate was subsequently introduced *via* bubbling for 5 min. The cell

was purged with Ar for 10 min, after which H<sub>2</sub> was introduced to assess the reduction of the adsorbed ethyl acetate over a period of 100 min. IR spectra were collected throughout this procedure at one-min intervals.

#### **1.4 Catalytic performance evaluation**

Catalytic conversion of PET was conducted using a PSK-6 micro-magnetic heating reactor (Nanjing Zhengxin Instrument Co., Ltd.). First, 20 mg catalyst, 24 mg PET, 6 mL 2-PrOH, and 24 mg tridecane (internal standard) were added. The reactor was purged 5 times with H<sub>2</sub>, pressurized to 3 MPa, and heated to the target temperature. Upon reaction completion, the reactor was rapidly cooled, and the catalyst was separated by centrifugation. Liquid products were analyzed using a SHIMADZU GC-2010 gas chromatograph equipped with a FID detector, with product identification confirmed by Agilent 8860-8977B GC-MS.

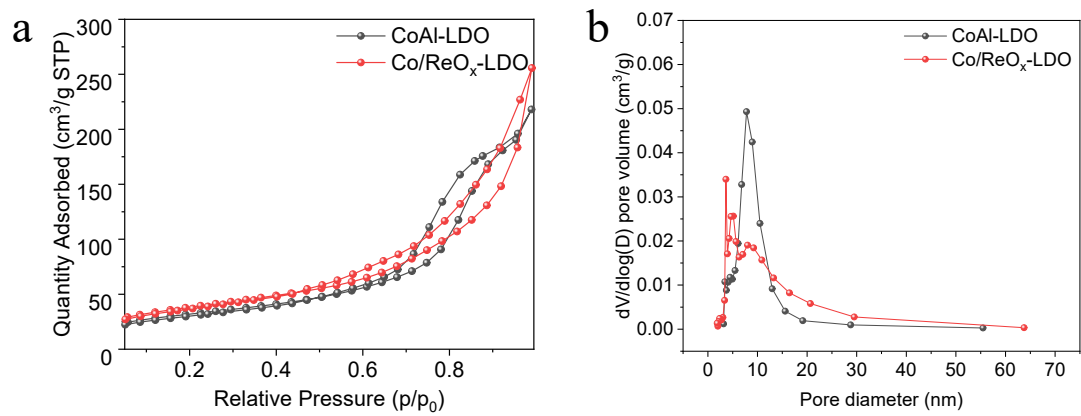


Fig. S1 (a) N<sub>2</sub> adsorption/desorption isotherms and (b) pore size distributions of Co/ReO<sub>x</sub>-LDO and CoAl-LDO.

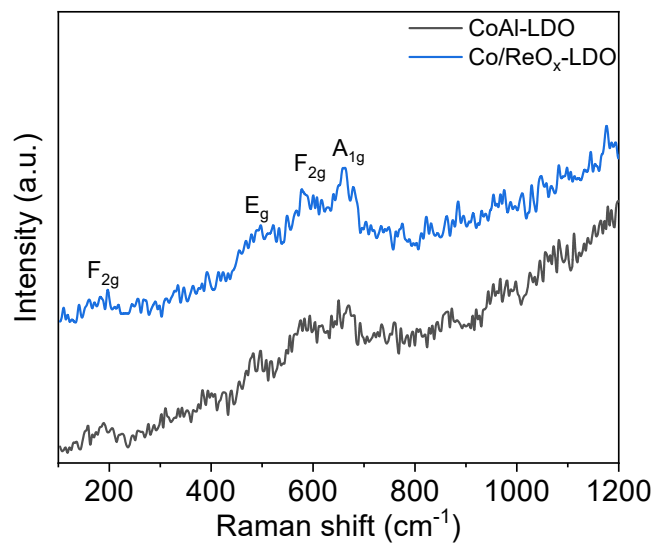


Fig. S2 Raman spectra of Co/ReO<sub>x</sub>-LDO and CoAl-LDO.

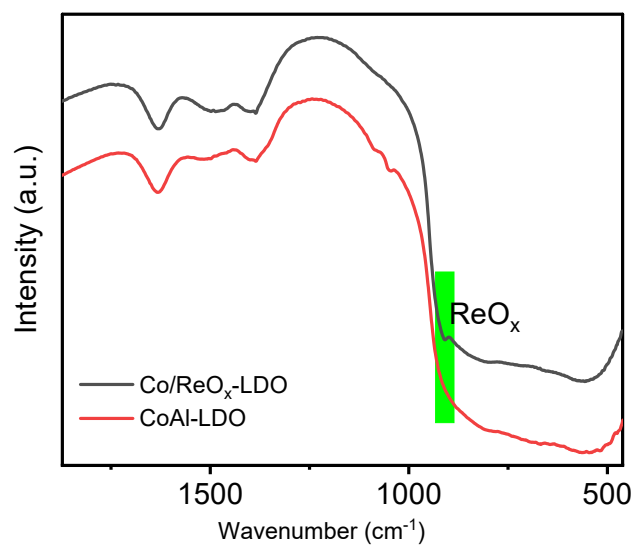


Fig. S3 FTIR spectra of Co/ReO<sub>x</sub>-LDO and CoAl-LDO.

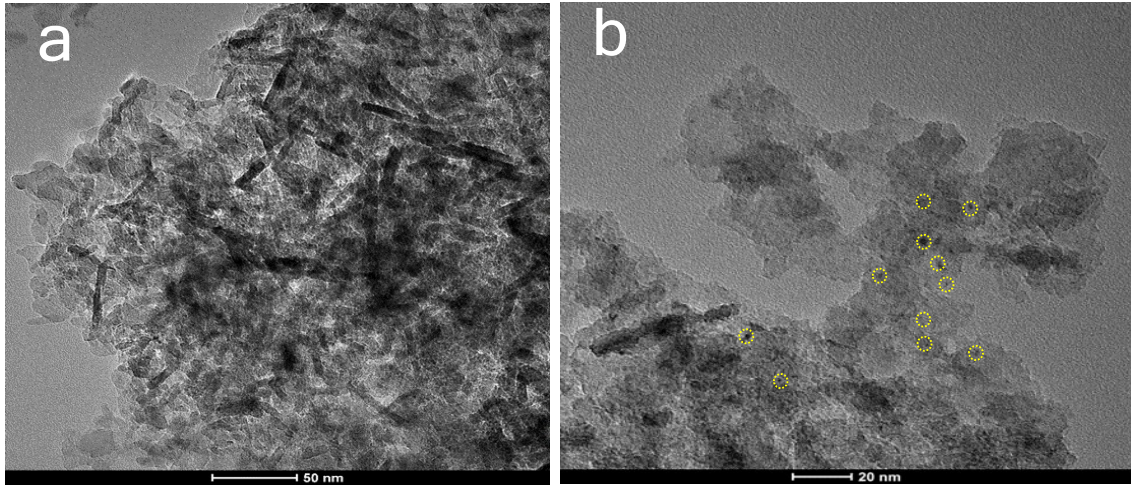


Fig. S4 (a, b) TEM images of  $\text{ReO}_x/\text{Al}_2\text{O}_3$ .

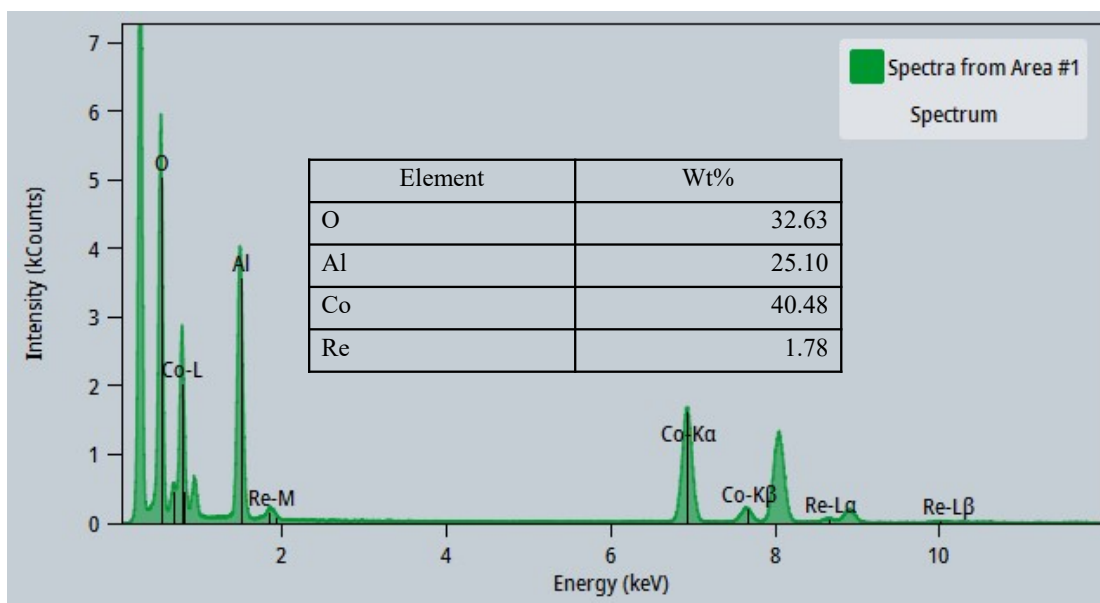


Fig. S5 EDX element analysis of Co/ReO<sub>x</sub>-LDO.

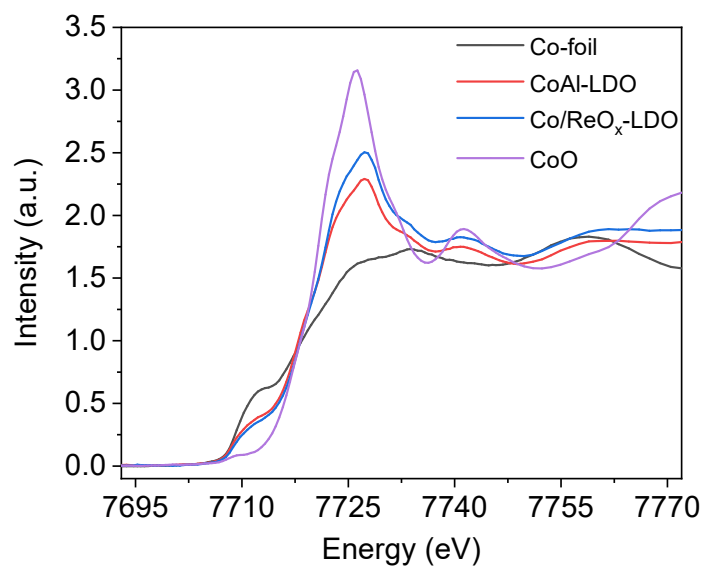


Fig. S6 XANES spectra of Co/ReO<sub>x</sub>-LDO and CoAl-LDO.

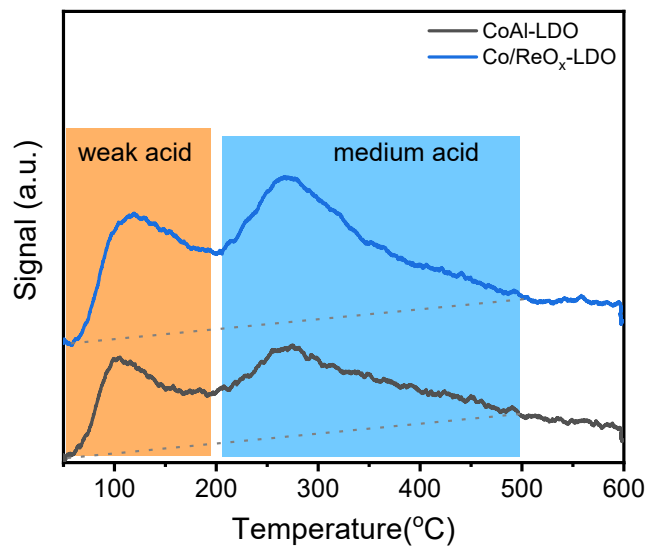


Fig. S7 NH<sub>3</sub>-TPD profiles of Co/ReO<sub>x</sub>-LDO and CoAl-LDO.

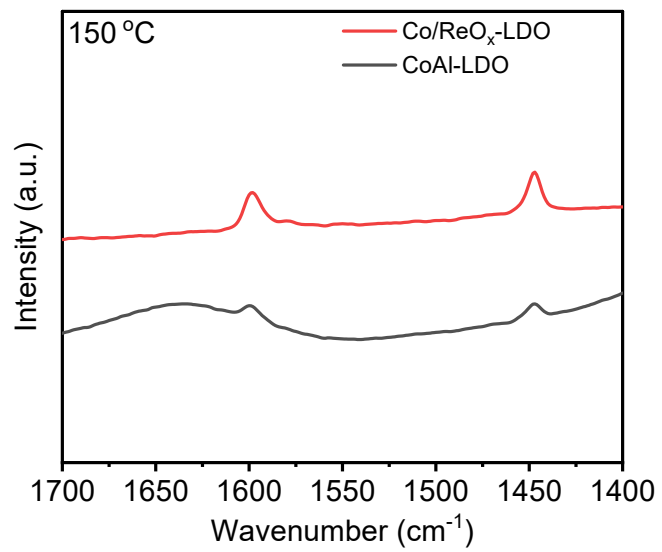


Fig. S8 Py-FTIR spectra of Co/ReO<sub>x</sub>-LDO and CoAl-LDO.

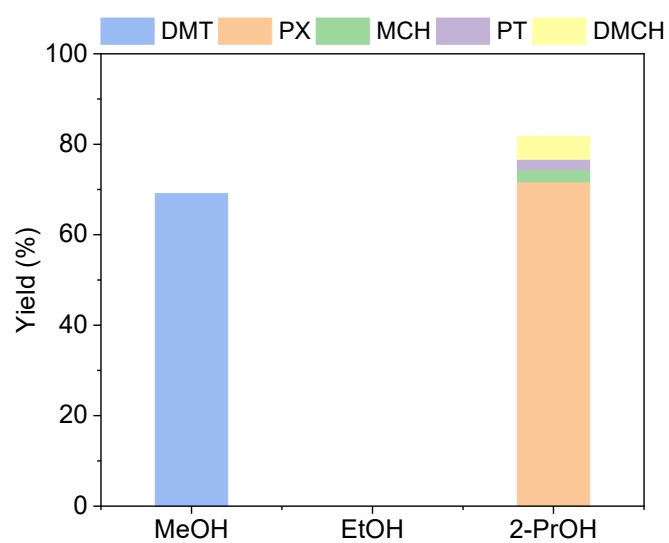


Fig. S9 The influence of solvent for PET conversion over Co/ReO<sub>x</sub>-LDO. Reaction conditions: 20 mg Co/ReO<sub>x</sub>-LDO, 24 mg PET, 6 mL solvent, 210 °C, 3 MPa H<sub>2</sub>.

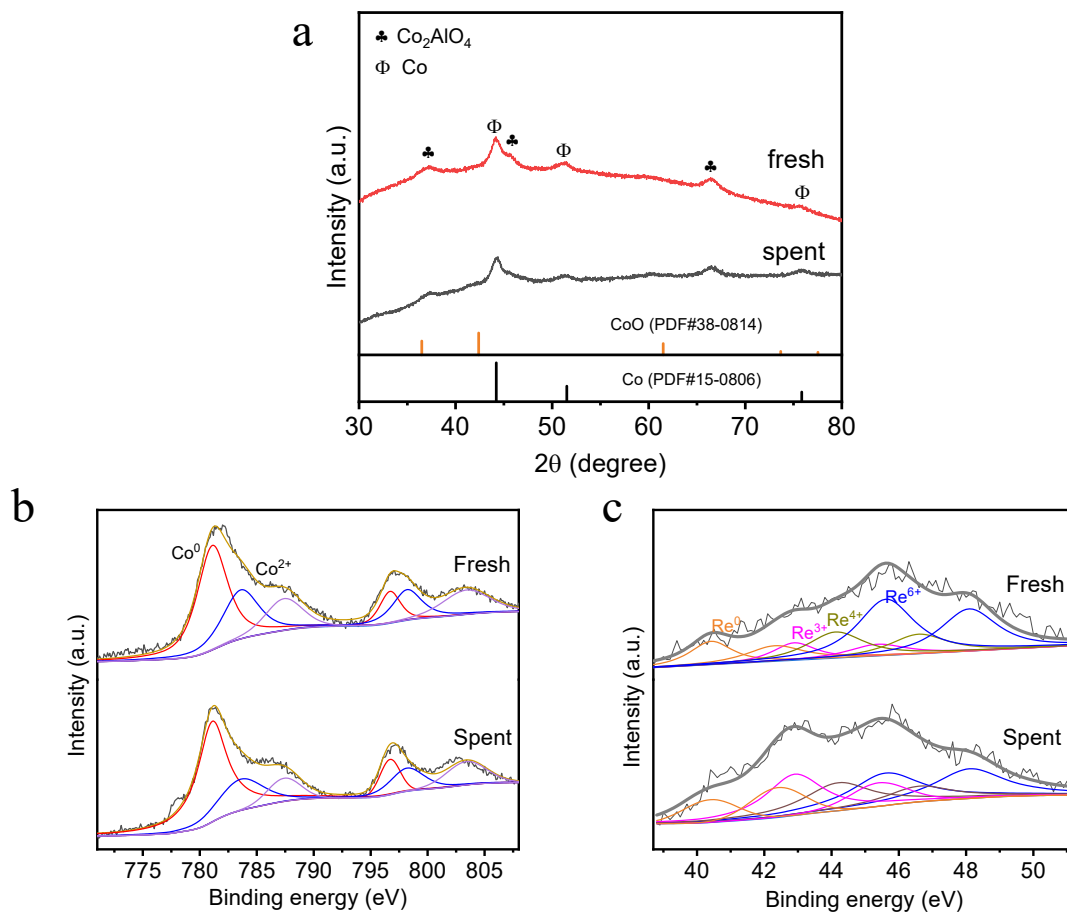


Fig. S10 (a) XRD patterns and (b, c) XPS spectra of fresh and spent Co/ReO<sub>x</sub>-LDO.

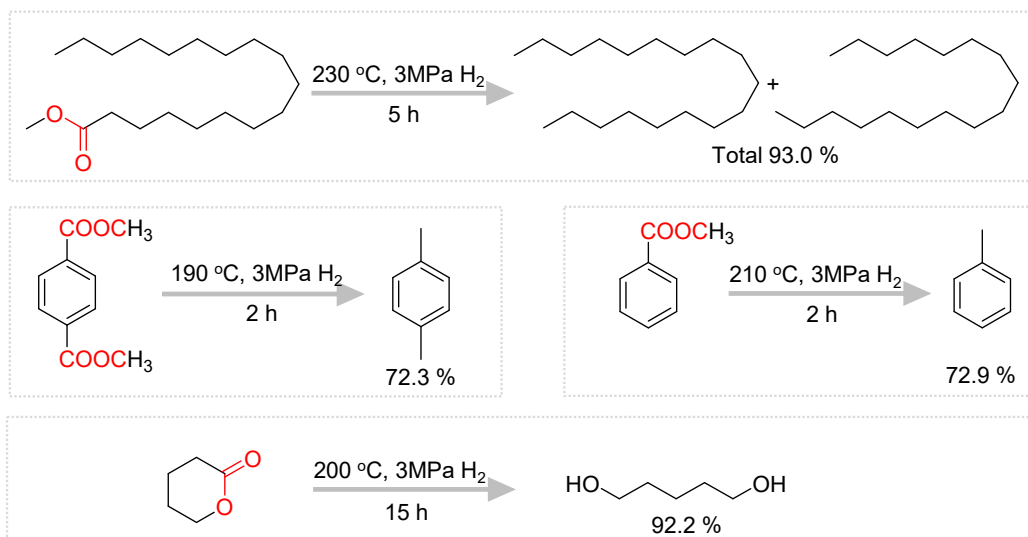


Fig. S11 Transformation of representative esters over Co/ReO<sub>x</sub>-LDO catalyst. Reaction conditions: methyl stearate (0.24 mmol), catalyst (40 mg), 2.5 mL 2-PrOH; DMT (0.14 mmol), catalyst (24 mg), 6 mL 2-PrOH; methyl benzoate (0.18 mmol), catalyst (40 mg), 6 mL 2-PrOH; ε-caprolactone (1 mmol), catalyst (40 mg), 3 mL 2-PrOH.

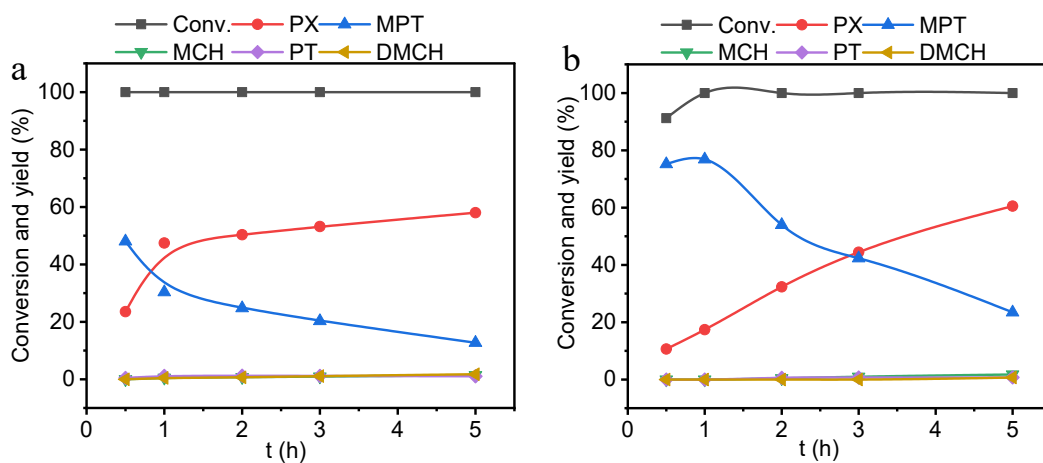


Fig. S12 Time profiles of DMT conversion over (a) Co/ReO<sub>x</sub>-LDO and (b) CoAl-LDO. Reaction conditions: 20 mg catalyst, 24 mg DMT, 6 mL 2-PrOH, 210 °C, 3 MPa H<sub>2</sub>.

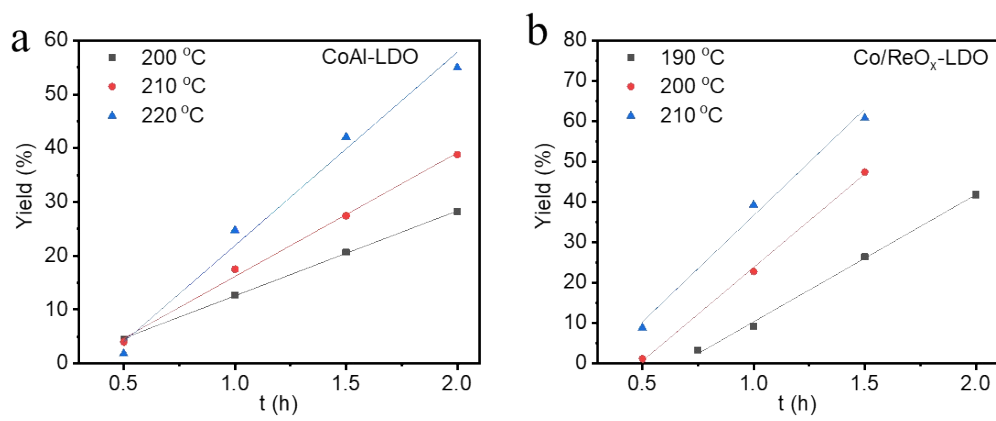


Fig. S13 Arrhenius plots for MB deoxygenation over (a) Co/ReO<sub>x</sub>-LDO and (b) CoAl-LDO. Reaction conditions: 5.3 mmol MB, 50 mg catalyst, 60 mL 2-PrOH, 3MPa H<sub>2</sub>.

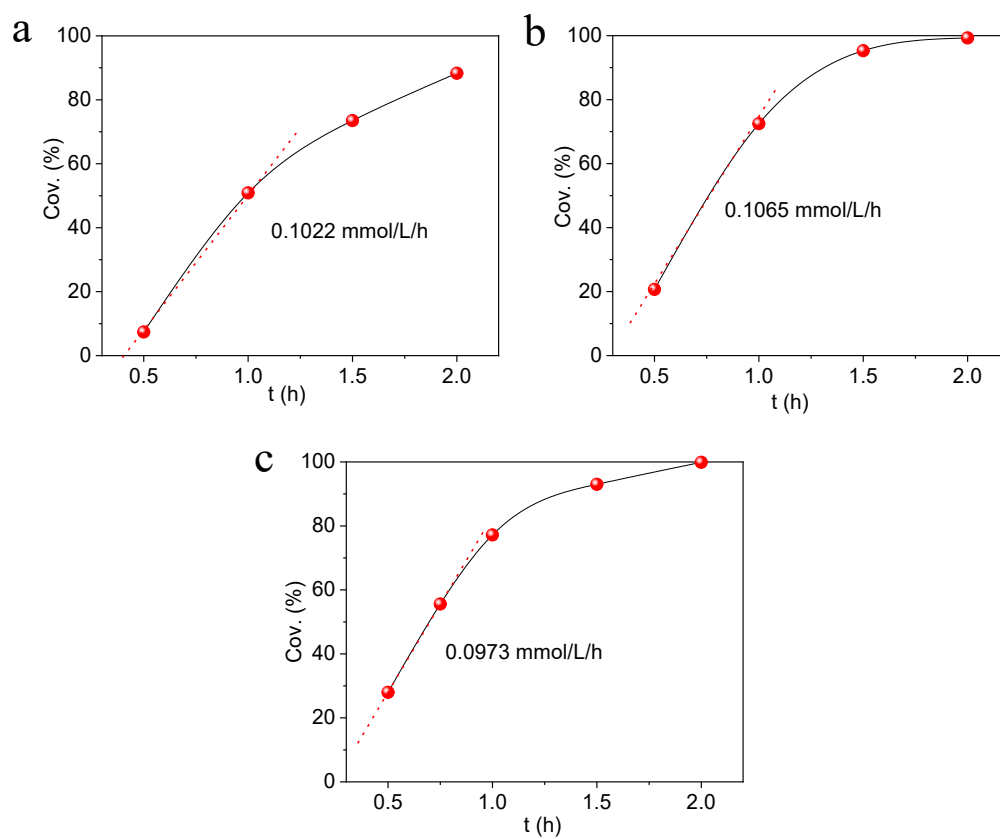


Fig. S14 Time profiles of MB deoxygenation at different MB concentration over Co-ReO<sub>x</sub>/LDO. Reaction conditions: (a) 5.3 mmol, (b) 4.6 mmol and (c) 4.0 mmol MB, 50 mg catalyst, 60 mL 2-PrOH, 3MPa H<sub>2</sub>.

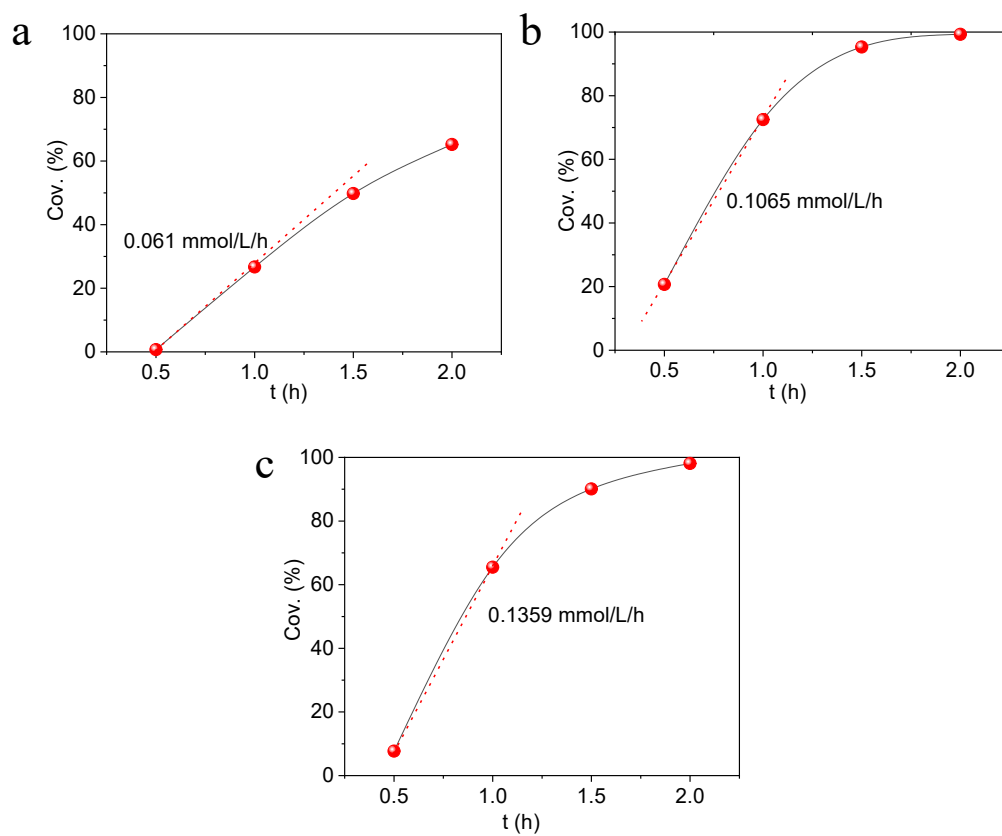


Fig. S15 Time profiles of MB deoxygenation at different  $H_2$  pressure over Co/ReO<sub>x</sub>-LDO. Reaction conditions: 5.3 mmol MB, 50 mg catalyst, 60 mL 2-PrOH, (a) 1 MPa  $H_2$ , (b) 2 MPa  $H_2$ , (c) 3 MPa  $H_2$ .

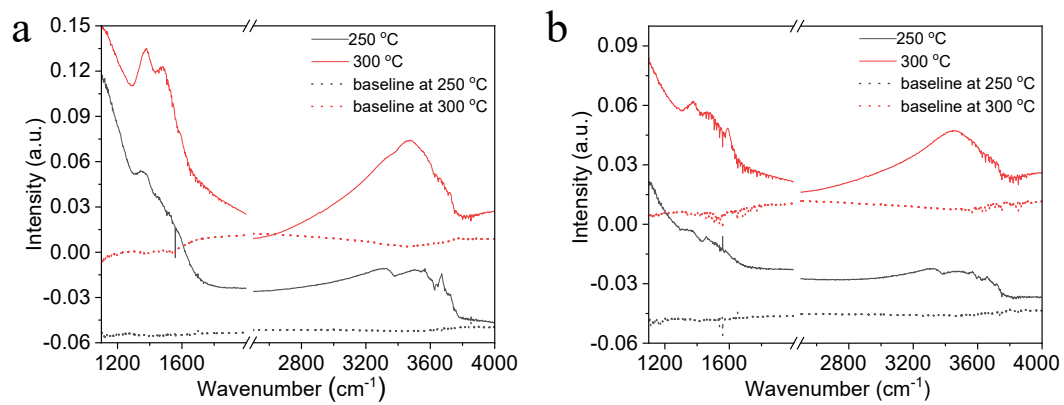


Fig. S16 In situ  $H_2$ -FTIR spectroscopy of (a) CoAl-LDO and (b) Co/ReO<sub>x</sub>-LDO at 250 and 300 °C.

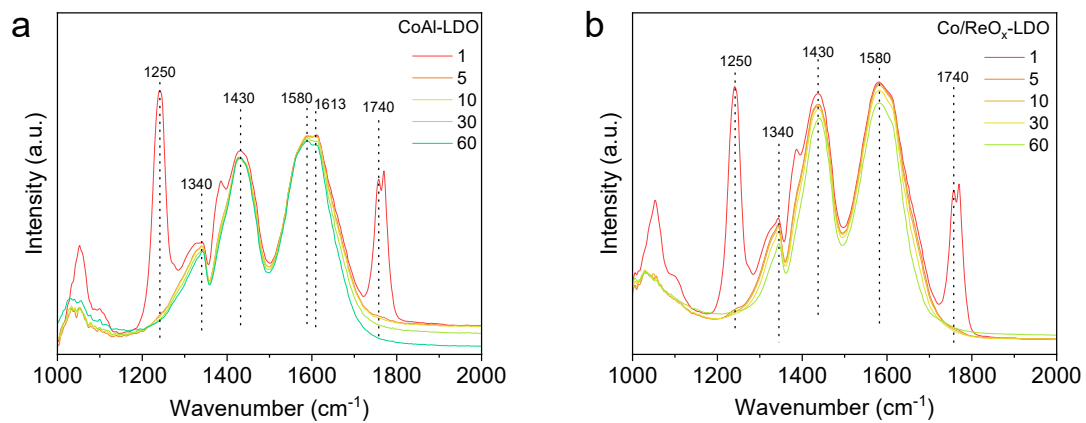


Fig. S17 In situ FTIR spectroscopy for ethyl acetate adsorption and Ar purge over (a) CoAl-LDO and (b) Co/ReO<sub>x</sub>-LDO.

Table S1 Pore parameters of various catalysts

Catalyst	$S_{\text{BET}}$ (m <sup>2</sup> /g) <sup>a</sup>	$V_{\text{total}}$ (cm <sup>3</sup> /g) <sup>b</sup>	Pore size (nm) <sup>c</sup>
CoAl-LDO	113	0.339	9.6
Co/ReO <sub>x</sub> -LDO	136	0.399	11.0

<sup>a</sup> Calculated using the Brunauer-Emmett-Teller (BET) method.

<sup>b</sup> Calculated using single-point adsorption at a relative pressure of 0.98.

<sup>c</sup> Calculated using the Barrett-Joyner-Halenda (BJH) method from the linear plot of desorption isotherms.

Table S2 The element content, crystal size, and surface species over Co/ReO<sub>x</sub>-LDO and CoAl-LDO.

Catalysts	Co loading (wt%) <sup>a</sup>	Re loading (wt%) <sup>a</sup>	Crystal size (nm) <sup>b</sup>	Particle size (nm) <sup>c</sup>	Dispersion (%) <sup>d</sup>	Relative percentage (at%) <sup>e</sup>	
						Co <sup>0</sup>	Co <sup>δ+</sup>
CoAl-LDO	25.2	-	10.6	15.6	6.4	38.1	61.9
Co/ReO <sub>x</sub> -LDO	28.9	4.3	7.0	6.1	16.4	54.0	46.0

<sup>a</sup> Determined by ICP-OES.

<sup>b</sup> Calculated by Scherrer Formula.

<sup>c</sup> Calculated from TEM images.

<sup>d</sup> Calculated with equation  $(1/d_{NP}) \times 100$ .

<sup>e</sup> Obtained from XPS fitting.

Table S3 PET hydrodeoxygenation over referenced catalysts.

Catalyst	Yield/%				Total aromatics	Total cycloalkanes	aromatic+cycloalkane	Aromatics distribution in hydrocarbon (%)
	PX	PT	MCH	DMCH				
none	0	0	0	0	0	0	0	0
Co/ReO <sub>x</sub> -LDO	71.7	2.3	2.7	5	74	7.7	81.7	90.6
Co-N-C-700 (2:1)	0.12	0	0	0	0.12	0	0.12	100
Co@NC	0.1	0	0	0	0.1	0	0.1	100
Ni <sub>2</sub> Al <sub>1</sub> -LDO	4.7	0.4	0.2	0.4	5.1	0.6	5.7	89.5
Cu/Al <sub>2</sub> O <sub>3</sub>	8.9	0	0	0	8.9	0	8.9	100
Fe/Al <sub>2</sub> O <sub>3</sub>	0.3	0	0	0	0.3	0	0.3	100
Ni/Al <sub>2</sub> O <sub>3</sub>	9.3	0	2.3	17.3	9.3	19.6	28.9	32.2

Reaction conditions: 20 mg catalyst, 24 mg PET, 6 mL 2-PrOH, 210 °C, 3 MPa H<sub>2</sub>, 4 h.

Table S4 Comparison of PET hydrodeoxygenation for PX production over representative noble and non-noble metal catalysts.

Catalyst	Substrate	T (°C)	Atmosphere & Pressure	Yield (%)	PX productivity (mmol/g <sub>-catal</sub> /h)	Catalyst stability	Ref.
Ru/Nb <sub>2</sub> O <sub>5</sub>	PET	220	N <sub>2</sub> , 2 MPa	16.6	0.1	<b>Unstable</b> , Need regeneration for next run	1
Ru/Nb <sub>2</sub> O <sub>5</sub>	PET	200	H <sub>2</sub> , 0.3 MPa	65	0.3	<b>Unstable</b> , Need regeneration for next run	2
Ru/TiO <sub>2</sub>	PET	230	H <sub>2</sub> , 0.3 MPa	4.3	0.01	Stable	3
Co/TiO <sub>2</sub>	TPA	340	H <sub>2</sub> , 3 MPa	87.9	N.D	<b>Unstable</b>	4
Cu <sub>1</sub> Zn <sub>2</sub> FeO <sub>x</sub>	PET	200	H <sub>2</sub> , 4 MPa	98.6	0.5	<b>Unstable</b>	5
Cu <sub>4</sub> Fe <sub>1</sub> Cr <sub>1</sub>	PET	240	CO <sub>2</sub> +H <sub>2</sub> , 3 M · Pa	49.3	0.1	Stable	6
Co-Fe-Al	PET	210	H <sub>2</sub> , 4 MPa	>99	0.4	Stable	7
CuNa/SiO <sub>2</sub>	PET	210	N <sub>2</sub> , 0.1 MPa	100	1.0	<b>Unstable</b>	8
<b>Co/ReO<sub>x</sub>- LDO</b>	<b>PET</b>	<b>210</b>	<b>H<sub>2</sub>, 3MPa</b>	<b>71.7</b>	<b>1.1</b>	<b>Stable</b>	<b>This work</b>

1. S. Lu, Y. Jing, B. Feng, Y. Guo, X. Liu and Y. Wang, *ChemSusChem*, 2021, **14**, 4242-4250.
2. Y. Jing, Y. Wang, S. Furukawa, J. Xia, C. Sun, M. J. Hülsey, H. Wang, Y. Guo, X. Liu and N. Yan, *Angew. Chem. Int. Ed.*, 2021, **60**, 5527-5535.
3. M. Ye, Y. Li, Z. Yang, C. Yao, W. Sun, X. Zhang, W. Chen, G. Qian, X. Duan, Y. Cao, L. Li, X. Zhou and J. Zhang, *Angew. Chem. Int. Ed.*, 2023, **62**, e202301024.
4. S. Hongkailers, Y. Jing, Y. Wang, N. Hinchiranan and N. Yan, *ChemSusChem*, 2021, **14**, 4330-4339.
5. Y. Shao, L. Kong, M. Fan, K. Sun, G. Gao, C. Li, L. Zhang, S. Zhang, Y. Wang and X. Hu, *ACS Sustainable Chem. Eng.*, 2024, **12**, 3818-3830.
6. Y. Li, M. Wang, X. Liu, C. Hu, D. Xiao and D. Ma, *Angew. Chem.*, 2022, **61**, e202117205.
7. Y. Shao, M. Fan, K. Sun, G. Gao, C. Li, D. Li, Y. Jiang, L. Zhang, S. Zhang and X. Hu, *Green Chem.*, 2023, **25**, 10513-10529.
8. Z. Gao, B. Ma, S. Chen, J. Tian and C. Zhao, *Nat Commun.*, 2022, **13**, 3343.